

Monolithic Homotopy Continuation with Predictor Based on Higher Derivatives

David A. Brown and David W. Zingg

University of Toronto Institute for Aerospace Studies, Toronto, Ontario, M3H 5T6, Canada

Abstract

The predictor component of a monolithic homotopy continuation algorithm is augmented with higher derivative information for use as an efficient, robust, and scalable continuation algorithm suitable for application to large sparse systems of nonlinear algebraic equations. Convergence of the algorithm is established analytically, and efficiency studies are performed by applying the method to a practical computational aerodynamics problem.

Keywords: homotopy, continuation, higher order predictor, globalization, Newton-Krylov, computational fluid dynamics

1. Introduction

Homotopy continuation methods are root-finding algorithms based on continuous deformations known as homotopies [1]. Some applications in the field of computational fluid dynamics (CFD) include the study systems where multiple solutions exist [29, 36] or where solutions may be unstable [18, 35]. Homotopy continuation has also been applied to facilitate the solution to CFD problems at high Reynolds numbers by solving the same problem at a lower Reynolds number and gradually increasing the Reynolds number [7].

Motivated (at least in some cases) by the increased demand for scalable CFD solvers, there has been interest in implementing homotopy continuation as an efficient equation solver for CFD problems in general [3, 14, 17] or with special focus on higher-order accurate spatial discretizations [34, 37]. By far the most common continuation method in CFD is pseudo-transient continuation, the computational cost of which scales super-linearly with mesh refinement due to the dependence on the Courant-Friedrichs-Lewy (CFL) number [22]. Homotopy continuation algorithms can fare better. For example, Hao *et al.* [14] found that computational cost scales linearly with mesh refinement for a homotopy continuation algorithm for some one- and two-dimensional problems for a third-order finite-difference WENO scheme [21], presumably using a direct solver. Brown and Zingg [6] similarly observed better performance scaling for some three-dimensional inviscid cases using a finite-difference SBP-SAT [8, 9, 12, 20] discretization with the Krylov linear solver FGMRES [30].

The present research programme follows from the work of Hicken *et al.* [15], who studied a non-physical homotopy based on adding a large amount of non-physical dissipation to the discrete governing equations and gradually removing it. Based on the promising results presented by the authors, we continued this approach using a predictor-corrector method [3], which was

later improved upon by introducing a more efficient monolithic approach to homotopy curve tracing [6].

The monolithic approach of Brown and Zingg [6] can be interpreted as combining the predictor and corrector components of the predictor-corrector algorithm into a single update. A Newton-like corrector was used to reduce error associated with the current homotopy estimate in conjunction with a tangent predictor, which is second-order accurate, to estimate progress of the homotopy. The current paper presents an augmented formulation of the monolithic homotopy continuation algorithm which allows for the inclusion of predictors based on higher derivatives.

Higher derivative information can be used to improve the accuracy in locally predicting the homotopy [5], but comes at increased computational cost. The only way to determine if this additional cost is justifiable is through numerical investigation. Aside from potential efficiency gains, utilizing higher derivatives in predicting the homotopy can potentially lead to improved algorithm robustness, as an algorithm based on the first derivative with a posteriori step-length adaptation has limited capability of anticipating or responding to sudden changes in the curvature of the homotopy. The objectives of this paper are to develop an augmented version of the monolithic homotopy continuation algorithm using higher curve derivatives, to develop a practical and efficient method for applying the algorithm, to establish convergence analytically, and to investigate the algorithm numerically.

2. Flow Solver

The flow solver to which the monolithic homotopy continuation algorithm is applied is a Newton-Krylov-Schur parallel implicit flow solver based on a finite-difference [22] discretization applicable to multi-block structured grids. The finite-difference discretization is based on the SBP-SAT [8, 9, 12, 20] approach, which uses Summation-By-Parts (SBP) operators to represent the discrete derivatives and Simultaneous Approximation Terms (SATs) to enforce the boundary conditions and couple the flow equations at block interfaces. The flow solver originated as an inviscid flow solver due to Hicken and Zingg [16] and was extended to the Reynolds-averaged Navier-Stokes equations by Osusky and Zingg [27], though only inviscid cases are considered in this paper.

To parallelize the flow solver, the domain is decomposed into blocks. Parallel preconditioning of the Krylov solver is performed using the Schur complement method [30] with block incomplete lower-upper (ILU) preconditioning applied to the domain blocks. The specific type of ILU factorization used in the current study is known as $ILU(p)$ [30], where p is the fill level. The $ILU(p)$ factorization is constructed based on an approximate Jacobian matrix using nearest neighbour nodes only. Since the Schur complement preconditioner can vary slightly throughout the Krylov solution process, a flexible variant of the Krylov solver GMRES is used, which is termed Flexible Generalized Minimal Residual, or FGMRES [30].

To avoid forming and storing the full Jacobian matrix, the matrix-vector products needed by the linear solver can be estimated using either the approximate Jacobian matrix used in forming the preconditioner in place of the full Jacobian or using a finite-differencing technique [19, 26]. The finite-differencing is more expensive but more accurate and is used for all studies in this paper.

3. Inexact Newton Method

Newton's method is a root-finding method with q super-linear convergence near the root [10], though only local convergence is generally expected. As such, it normally needs to be *globalized* using a globally convergent method such as pseudo-transient continuation or the homotopy method. *Globalization* is the determination of a point sufficiently near the solution that a root-finding algorithm is expected to converge.

Consider a nonlinear algebraic system of equations, represented by

$$\mathcal{F}(\mathbf{x}) = \mathbf{0}, \quad (1)$$

$$\mathcal{F} : \mathbb{R}^N \rightarrow \mathbb{R}^N, \mathbf{x} \in \mathbb{R}^N.$$

The update due to Newton's method, when applied to this system of equations, is calculated by solving the linear system of equations

$$\nabla \mathcal{F}(\mathbf{x}_i) \Delta \mathbf{x}_i = -\mathcal{F}(\mathbf{x}_i), \quad (2)$$

$$\Delta \mathbf{x}_i \equiv \mathbf{x}_{i+1} - \mathbf{x}_i,$$

where $\nabla \mathcal{F}(\mathbf{x}_i) : \mathbb{R}^N \rightarrow \mathbb{R}^N$ is the Jacobian of $\mathcal{F}(\mathbf{x}_i)$, defined as

$$\nabla \mathcal{F}_{[j,k]}(\mathbf{x}) \equiv \frac{\partial \mathcal{F}_{[j]}(\mathbf{x})}{\partial \mathbf{x}_{[k]}}, \quad (3)$$

where the subscripted square brackets indicate a matrix or vector index and the non-bracketed subscripts denote the iteration index. The Jacobian of \mathcal{F} can be represented by a square matrix.

If the linear system (2) is being solved to some relative tolerance $\tau_{1,i} \in \mathbb{R}$, as in the results presented in this paper, then the actual Newton step is taken inexactly, and the update $\Delta \mathbf{x}_i$ does not satisfy equation (2) but does satisfy the inequality

$$\|\mathcal{F}(\mathbf{x}_i) + \nabla \mathcal{F}(\mathbf{x}_i) \Delta \mathbf{x}_i\| \leq \tau_{1,i} \|\mathcal{F}(\mathbf{x}_i)\|. \quad (4)$$

4. Convex Homotopy Continuation

Consider a nonlinear system of equations (1) as well as the so-called *convex homotopy* [1] which is defined as the (presumably) continuous isolated solution $\mathbf{x}_s : \mathbb{R} \rightarrow \mathbb{R}^N, (\lambda) \mapsto \mathbf{x}_s(\lambda), \lambda \in \mathbb{R}$ to

$$\mathcal{H}(\mathbf{x}, \lambda) = (1 - \lambda) \mathcal{F}(\mathbf{x}) + \lambda \mathcal{G}(\mathbf{x}) = \mathbf{0}, \quad (5)$$

$$\mathcal{H} : \mathbb{R}^N \times \mathbb{R} \rightarrow \mathbb{R}^N, \mathcal{G} : \mathbb{R}^N \rightarrow \mathbb{R}^N, \mathcal{F} : \mathbb{R}^N \rightarrow \mathbb{R}^N,$$

$$\lambda \in \Lambda, \Lambda = \{\lambda \in \mathbb{R}, \lambda \in [0, 1]\}$$

Interpreting the homotopy as a curve existing in \mathbb{R}^N , a continuation method, called convex homotopy continuation, can be developed from this homotopy by discretizing in λ to form a sequence of nonlinear equations:

$$\mathcal{H}(\mathbf{x}, \lambda_i) = (1 - \lambda_i) \mathcal{F}(\mathbf{x}) + \lambda_i \mathcal{G}(\mathbf{x}) = \mathbf{0}, \quad (6)$$

$$\mathcal{H} : \mathbb{R}^N \times \mathbb{R} \rightarrow \mathbb{R}^N, \mathcal{G} : \mathbb{R}^N \rightarrow \mathbb{R}^N, \mathcal{F} : \mathbb{R}^N \rightarrow \mathbb{R}^N$$

$$i \in [0, m], \lambda_i \in \Lambda, \Lambda = \{\lambda \in \mathbb{R}, \lambda \in [0, 1]\}, \lambda_0 = 1, \lambda_m = 0, \lambda_{i+1} < \lambda_i.$$

Solving $\mathcal{H}(\mathbf{x}, \lambda) = \mathbf{0}$ for sequentially increasing i is referred to as *traversing*.

It can also be of interest to formulate convex homotopy continuation in terms of an arbitrary parametrization, in which case equations (5) and (6) are unmodified but the solution is interpreted as the pair

$$(s) \mapsto \mathbf{x}_s(s), (s) \mapsto \lambda(s), \\ \mathbf{x} : \mathbb{R} \rightarrow \mathbb{R}^N, \lambda : \mathbb{R} \rightarrow \mathbb{R}, s \in \mathbb{S}, \mathbb{S} \subset \mathbb{R}.$$

This pair can be conveniently represented as a single function

$$c \in \mathbb{R}^{N+1}, (s) \mapsto c(s), c(s) \equiv [\mathbf{x}(s); \lambda(s)].$$

Choice of parametrization does not affect the continuous curve but can influence some step-length adaptation strategies used in the discrete algorithm. Most commonly, an arc-length parametrization is used [1], which is defined implicitly by

$$\|\dot{c}(s)\| = 1. \quad (7)$$

In this paper it is assumed that the curve is *regular*, which is to say that the Jacobian of \mathcal{H} is nonsingular for all λ , which also indicates that no bifurcations are present [1]. While bifurcation study is often of interest, it is not relevant to our objectives and regularity is consistent with our experience with the homotopies relevant to our applications.

5. Monolithic Homotopy Continuation

In this section the original formulation of the monolithic homotopy continuation algorithm presented previously by Brown and Zingg [6] is reviewed.

5.1. Continuous Form

The monolithic homotopy continuation algorithm is constructed based on the dynamic inversion principle. Consider a regular homotopy

$$\mathcal{H}(\mathbf{x}, \lambda) = \mathbf{0} \quad (8)$$

$\mathcal{H} : \mathbb{R}^N \times \mathbb{R} \rightarrow \mathbb{R}^N$, $(\mathbf{x}, \lambda) \mapsto \mathcal{H}(\mathbf{x}, \lambda)$ with parameter $\lambda \in \mathbb{R}$ and solution curve $\mathbf{x}_s(\lambda)$. The idea behind dynamic inversion is that it may be possible to construct a *dynamic inverse* $\mathcal{H}^* : \mathbb{R}^N \times \mathbb{R} \rightarrow \mathbb{R}^N$, $(\mathbf{w}, \lambda) \mapsto \mathcal{H}^*(\mathbf{w}, \lambda)$ such that the solution to the ordinary differential equation (ODE)

$$\dot{\mathbf{x}}(\lambda) + \mathcal{H}^*(\mathcal{H}(\mathbf{x}, \lambda), \lambda) = \mathbf{0} \quad (9)$$

is locally asymptotically convergent to $\mathbf{x}_s(\lambda)$. The formal definition of the dynamic inverses in the context of a homotopy with arbitrary parametrization is as follows.

Definition 1. Let $\mathbf{x}_s(\lambda)$ be a regular homotopy defined implicitly by $\mathcal{H}(\mathbf{x}, \lambda) = \mathbf{0}$, $\mathcal{H} : \mathbb{R}^N \times \mathbb{R} \rightarrow \mathbb{R}^N$. Let $\mathcal{H}^* : \mathbb{R}^N \times \mathbb{R} \rightarrow \mathbb{R}^N$ be continuous on the ball

$$\mathcal{B}_r(\mathbf{x}_s) \equiv \left\{ \mathbf{x} \in \mathbb{R}^N \mid \mathbf{x} = \mathbf{x}_s + \Delta\mathbf{x}, r > 0, \|\Delta\mathbf{x}\| \leq r \right\}. \quad (10)$$

Then \mathcal{H}^* is called a forward dynamic inverse of \mathcal{H} on $\mathcal{B}_r(\mathbf{x}_s)$ if there exists fixed $\beta \in \mathbb{R}$, $0 < \beta < \infty$, such that

$$\Delta \mathbf{x}^T \mathcal{H}^*(\mathcal{H}(\mathbf{x}_s + \Delta \mathbf{x}, \lambda), \lambda) \geq \beta \|\Delta \mathbf{x}\|^2 \quad (11)$$

for all $\mathbf{x} \in \mathcal{B}_r(\mathbf{x}_s)$.

Definition 2. Let $\mathbf{x}_s(s)$ be a regular homotopy defined implicitly by $\mathcal{H}(\mathbf{x}(s), \lambda(s)) = \mathbf{0}$, $\mathcal{H} : \mathbb{R}^N \times \mathbb{R} \rightarrow \mathbb{R}^N$. Let $\mathcal{H}^* : \mathbb{R}^N \times \mathbb{R} \rightarrow \mathbb{R}^N$ be continuous on the ball $\mathcal{B}_r(\mathbf{x}_s)$ defined by equation (10). Then \mathcal{H}^* is called a reverse mode dynamic inverse of \mathcal{H} on $\mathcal{B}_r(\mathbf{x}_s)$ if there exists fixed $\beta \in \mathbb{R}$, $0 < \beta < \infty$, such that

$$\Delta \mathbf{x}^T \mathcal{H}^*(\mathcal{H}(\mathbf{x}_s + \Delta \mathbf{x}, \lambda), \lambda) \leq -\beta \|\Delta \mathbf{x}\|^2 \quad (12)$$

for all $\mathbf{x} \in \mathcal{B}_r(\mathbf{x}_s)$.

Remark 1. If \mathcal{H}^* is a dynamic inverse of \mathcal{H} with constant β , then for any $\gamma \in \mathbb{R}$, $\gamma > 0$, $\gamma \mathcal{H}^*$ is a dynamic inverse of \mathcal{H} with constant $\gamma\beta$.

Remark 2. If \mathcal{H}^* is a forward dynamic inverse of \mathcal{H} , then $-\mathcal{H}^*$ is a reverse mode dynamic inverse of \mathcal{H} .

In the context of homotopy, either the forward or reverse version of the dynamic inverse is applied depending on which direction the curve is being traversed. The following two theorems assert, for each case, convergence to the curve for an ODE constructed from the appropriate dynamic inverse and an estimate of the tangent vector.

Theorem 1. Let $\mathbf{x}_s(\lambda)$ be a regular homotopy defined implicitly by $\mathcal{H}(\mathbf{x}(\lambda), \lambda(\lambda)) = \mathbf{0}$. Let $\mathcal{H}^* : \mathbb{R}^N \times \mathbb{R} \rightarrow \mathbb{R}^N$; $(\mathbf{w}, \lambda) \mapsto \mathcal{H}^*(\mathbf{w}, \lambda)$ be a forward dynamic inverse of $\mathcal{H}(\mathbf{x}, \lambda)$ on $\mathcal{B}_r(\mathbf{x}_s)$. Let $\mathcal{E} : \mathbb{R}^N \times \mathbb{R} \rightarrow \mathbb{R}^N$; $(\mathbf{x}, \lambda) \mapsto \mathcal{E}(\mathbf{x}, \lambda)$ be locally Lipschitz in \mathbf{x} and λ such that for some fixed $\omega \in (0, \infty)$, $\mathcal{E}(\mathbf{x}, \lambda)$ satisfies

$$-\frac{1}{2}\omega \|\Delta \mathbf{x}(\lambda)\|^2 \leq \Delta \mathbf{x}(\lambda)^T [\mathcal{E}(\mathbf{x}_s(\lambda) + \Delta \mathbf{x}(\lambda), \lambda) + \dot{\mathbf{x}}_s(\lambda)] \leq \frac{1}{2}\omega \|\Delta \mathbf{x}(\lambda)\|^2 \quad (13)$$

for all $\mathbf{x}_s + \Delta \mathbf{x} \in \mathcal{B}_r(\mathbf{x}_s)$. Let $\mathbf{x} = \mathbf{x}_s + \Delta \mathbf{x}$ satisfy

$$-\dot{\mathbf{x}}(\lambda) = -\gamma \mathcal{H}^*(\mathcal{H}(\mathbf{x}(\lambda), \lambda), \lambda) + \mathcal{E}(\mathbf{x}(\lambda), \lambda), \quad (14)$$

where $\gamma \in \mathbb{R}$, $\gamma > 0$ (see Remark 1). Consider now some $\lambda_k \in \mathbb{R}$ with corresponding $\mathbf{x}(\lambda_k) \in \mathcal{B}_r(\mathbf{x}_s(\lambda))$. Then

$$\|\mathbf{x}(\lambda) - \mathbf{x}_s(\lambda)\| \leq \|\mathbf{x}(\lambda_k) - \mathbf{x}_s(\lambda_k)\| e^{-(\gamma\beta - \omega)(\lambda - \lambda_k)} \quad (15)$$

for all $\lambda > \lambda_k$.

Proof. Getz [13] pp. 32-33. □

Theorem 2. Let $\mathbf{x}_s(\lambda)$ be a regular homotopy defined implicitly by $\mathcal{H}(\mathbf{x}(\lambda), \lambda(\lambda)) = \mathbf{0}$. Let $\mathcal{H}^* : \mathbb{R}^N \times \mathbb{R} \rightarrow \mathbb{R}^N$; $(\mathbf{w}, \lambda) \mapsto \mathcal{H}^*(\mathbf{w}, \lambda)$ be a reverse-mode dynamic inverse of $\mathcal{H}(\mathbf{x}, \lambda)$ on $\mathcal{B}_r(\mathbf{x}_s)$. Let $\mathcal{E} : \mathbb{R}^N \times \mathbb{R} \rightarrow \mathbb{R}^N$; $(\mathbf{x}, \lambda) \mapsto \mathcal{E}(\mathbf{x}, \lambda)$ be locally Lipschitz in \mathbf{x} and λ such that for some fixed $\omega \in (0, \infty)$, $\mathcal{E}(\mathbf{x}, \lambda)$ satisfies equation (13) for all $\mathbf{x}_s + \Delta \mathbf{x} \in \mathcal{B}_r(\mathbf{x}_s)$. Let $\mathbf{x} = \mathbf{x}_s + \Delta \mathbf{x}$ satisfy

$$-\dot{\mathbf{x}}(\lambda) = \gamma \mathcal{H}^*(\mathcal{H}(\mathbf{x}(\lambda), \lambda), \lambda) + \mathcal{E}(\mathbf{x}(\lambda), \lambda), \quad (16)$$

where $\gamma \in \mathbb{R}$, $\gamma > 0$ (see Remark 1). Consider now some $\lambda_k \in \mathbb{R}$ with corresponding $\mathbf{x}(\lambda_k) \in \mathcal{B}_r(\mathbf{x}_s(\lambda))$. Then

$$\|\mathbf{x}(\lambda) - \mathbf{x}_s(\lambda)\| \leq \|\mathbf{x}(\lambda_k) - \mathbf{x}_s(\lambda_k)\| e^{-(\gamma\beta - \omega)(\lambda_k - \lambda)} \quad (17)$$

for all $\lambda < \lambda_k$.

Proof. Brown and Zingg [6] pp. 61-62. \square

5.2. Discrete Form

The monolithic homotopy continuation algorithm is developed by numerically integrating either equation (14) or (16) in the forward or reverse direction, as appropriate. Integration of a differential equation refers to its approximate numerical evaluation. In the present case this is performed using forward Euler parameter integration. The following theorem will be important in the analysis.

Theorem 3. *Suppose that the ODE*

$$\dot{\mathbf{x}}(\lambda) + \mathcal{H}(\mathbf{x}(\lambda), \lambda) = \mathbf{0}$$

with $\mathcal{H} : \mathbb{R}^N \times \mathbb{R} \rightarrow \mathbb{R}^N$ and initial condition $\mathbf{x} = \mathbf{x}_0$ has unique C^2 solution. Define $\Delta\lambda_i \equiv \lambda_{i+1} - \lambda_i$. Then the forward Euler integration of this ODE, given by

$$\mathbf{x}_{i+1} - \mathbf{x}_i + \Delta\lambda_i \mathcal{H}(\mathbf{x}(\lambda_i), \lambda_i) = \mathbf{0},$$

converges to the solution of the ODE in the limit of $\Delta\lambda_i \rightarrow 0$.

Proof. This is established in numerous textbooks, including Lomax *et al.* [22], Chapter 6. \square

Application of forward Euler parameter integration to the forward dynamic inverse ODE (14) in the direction of increasing λ yields

$$\mathbf{x}_{i+1} = \mathbf{x}_i - \Delta\lambda_i \gamma \mathcal{H}^*(\mathcal{H}(\mathbf{x}(\lambda_i), \lambda_i), \lambda_i) + \Delta\lambda_i \mathcal{E}(\mathbf{x}(\lambda_i), \lambda_i) \quad (18)$$

where $\Delta\lambda_i > 0$. Application of forward Euler parameter integration to the reverse-mode dynamic inverse ODE (16) in the direction of decreasing λ yields

$$\mathbf{x}_{i+1} = \mathbf{x}_i + \Delta\lambda_i \gamma \mathcal{H}^*(\mathcal{H}(\mathbf{x}(\lambda_i), \lambda_i), \lambda_i) + \Delta\lambda_i \mathcal{E}(\mathbf{x}(\lambda_i), \lambda_i) \quad (19)$$

where $\Delta\lambda_i < 0$.

5.3. Nearby Inverse Jacobian as Dynamic Inverse

The inverse Jacobian forms a dynamic inverse [13]. Since points on the curve are approximated, rather than solved for exactly, it is important to establish that the Jacobian continues to function as a dynamic inverse when evaluated at a point sufficiently near to the curve. This is formalized in the following theorem.

Theorem 4. *Let $\mathbf{x}_s(\lambda)$ be a continuous isolated solution of $\mathcal{H}(\mathbf{x}, \lambda) = \mathbf{0}$. Assume that $\mathcal{H}(\mathbf{x}, \lambda)$ is C^∞ in both \mathbf{x} and λ on $\mathcal{B}_r(\mathbf{x}_s)$ and that $\nabla_{\mathbf{x}} \mathcal{H}(\mathbf{x}, \lambda)$ is nonsingular at and near to \mathbf{x}_s . Then for any $0 < \beta < 1$ there exists r such that*

$$\mathcal{H}^*(\mathbf{w}, \lambda) = [\nabla_{\mathbf{x}} \mathcal{H}(\mathbf{x}, \lambda)]^{-1} \mathbf{w} \quad (20)$$

is a dynamic inverse operating on $\mathbf{w} \in \mathbb{R}^N$ with parameter $\beta \in \mathbb{R}$ as defined in Theorem 1 for all $\mathbf{x} \in \mathcal{B}_r(\mathbf{x}_s(\lambda))$.

Proof. Getz [13], page 23. □

Remark 3. By Theorem 4 and Remark 2,

$$\mathcal{H}^*(\mathbf{w}, \lambda) = -[\nabla_{\mathbf{x}} \mathcal{H}(\mathbf{x}, \lambda)]^{-1} \mathbf{w} \quad (21)$$

is a reverse-mode dynamic inverse of $\mathcal{H}(\mathbf{x}, \lambda)$.

6. The Augmented Monolithic Homotopy Continuation Algorithm

The monolithic homotopy continuation algorithm of Section 5 is augmented by including higher curve derivative information in the update. The analysis of the augmented algorithm proceeds differently than the original formulation presented in Section 5. The inclusion of higher curve derivatives does not improve convergence of the continuous case but improves the prediction capabilities of the forward Euler integration. Therefore, we establish convergence by studying the discrete form of the equations directly.

The analysis begins by showing that points near to the homotopy curve lie on neighbouring homotopies which can be represented locally by Taylor series based on the original homotopy. Furthermore, the difference between these homotopies and the original varies continuously as a function of λ .

Theorem 5. Let $\mathbf{x}_s(\lambda)$ be a continuous isolated solution to $\mathcal{H}(\mathbf{x}, \lambda) = \mathbf{0}$, $\mathcal{H} : \mathbb{R}^N \times \mathbb{R} \rightarrow \mathbb{R}^N$. Let $\mathbf{x}'_s(\lambda)$ satisfy

$$\mathcal{H}'(\mathbf{x}, \lambda) \equiv \mathcal{H}(\mathbf{x}, \lambda) - \mathcal{K} = \mathbf{0}, \quad (22)$$

where $\mathcal{K} : \mathbb{R}^N \rightarrow \mathbb{R}^N$, $\mathcal{K} = \mathcal{H}(\mathbf{x}_0, \lambda_0)$ for some fixed $\mathbf{x}_0 \in \mathbb{R}^N$, $\lambda_0 \in \mathbb{R}$, $0 < \lambda_0 < 1$. Assume that $\mathcal{H} : \mathbb{R}^N \times \mathbb{R} \rightarrow \mathbb{R}^N$ is continuous with nonsingular Jacobian along $\mathbf{x}_s(\lambda)$ and $\mathbf{x}'_s(\lambda)$. Define $\Delta \mathbf{x} \equiv \mathbf{x}'_s(\lambda) - \mathbf{x}_s(\lambda)$ and let $\varepsilon \in \mathbb{R}$, $\delta \in \mathbb{R}$. Then $\forall \varepsilon > 0$, $\exists \delta > 0$ such that

$$|\Delta \mathbf{x}(\lambda + \delta)^T \Delta \mathbf{x}(\lambda + \delta) - \Delta \mathbf{x}(\lambda)^T \Delta \mathbf{x}(\lambda)| < \varepsilon. \quad (23)$$

Proof. By the definition of continuity:

$$\begin{aligned} \forall \varepsilon > 0 \quad \exists \delta > 0 \text{ s.t. } & \begin{cases} \|\mathbf{x}'_s(\lambda + \delta) - \mathbf{x}'_s(\lambda)\| < \sqrt{\frac{1}{2}\varepsilon} \\ \|\mathbf{x}_s(\lambda + \delta) - \mathbf{x}_s(\lambda)\| < \sqrt{\frac{1}{2}\varepsilon} \end{cases} \\ \Rightarrow \|\mathbf{x}'_s(\lambda + \delta) - \mathbf{x}'_s(\lambda)\|^2 + \|\mathbf{x}_s(\lambda + \delta) - \mathbf{x}_s(\lambda)\|^2 & < \varepsilon \\ \Rightarrow \|\mathbf{x}'_s(\lambda + \delta) - \mathbf{x}'_s(\lambda) - \mathbf{x}_s(\lambda + \delta) + \mathbf{x}_s(\lambda)\|^2 & < \varepsilon \\ \Rightarrow \|\Delta \mathbf{x}(\lambda + \delta) - \Delta \mathbf{x}(\lambda)\|^2 & < \varepsilon \\ \Rightarrow \|\Delta \mathbf{x}(\lambda + \delta)\|^2 - \|\Delta \mathbf{x}(\lambda)\|^2 & < \varepsilon, \end{aligned} \quad (24)$$

which is equivalent to equation (23). □

We now proceed to establish convergence for the augmented monolithic homotopy continuation algorithm, where the tangent vector appearing in the original algorithm is replaced with a Taylor expansion of degree n . The Taylor expansion comprises the tangent vector, curvature vector, and, potentially, higher derivatives as well. The forward version of the algorithm with $\lambda(s) = 1$ parametrization is presented first.

Theorem 6. Let $\mathbf{x}_s(\lambda)$ be a continuous isolated solution of a regular homotopy $\mathcal{H}(\mathbf{x}, \lambda) = \mathbf{0}$, $\mathcal{H} : \mathbb{R}^N \times \mathbb{R} \rightarrow \mathbb{R}^N$. Assume that $\mathcal{H}(\mathbf{x}, \lambda)$ is C^∞ in both \mathbf{x} and λ . Let $\mathcal{H}^*(\mathbf{w}, \lambda) = [\nabla_{\mathbf{x}} \mathcal{H}(\mathbf{x}, \lambda)]^{-1} \mathbf{w}$ be a forward dynamic inverse of $\mathcal{H}(\mathbf{x}, \lambda)$ on $\mathcal{B}_r(\mathbf{x}_s(\lambda))$. Then for sufficiently small $\Delta\lambda_i \equiv \lambda_{i+1} - \lambda_i > 0$ and for any $\frac{2}{3} < \gamma_i \Delta\lambda_i \leq 1$ there exists $\mathcal{B}_r(\mathbf{x}_s(\lambda))$ such that the difference equation

$$\mathbf{x}_{i+1} = \mathbf{x}_i - \gamma_i \Delta\lambda_i \mathcal{H}^*(\mathcal{H}(\mathbf{x}_i, \lambda_i), \lambda_i) + \sum_{k=1}^n \frac{1}{k!} \Delta\lambda_i^k \mathbf{x}^{(k)}(\lambda_i) \quad (25)$$

converges to $\mathbf{x}_s(\lambda)$ for any $n \geq 1$, where the bracketed superscript indicates differentiation.

Proof. Let $\mathbf{x}'(\lambda) \equiv \mathbf{x}_s(\lambda) + \mathbf{x}_i - \mathbf{x}_s(\lambda_i)$ and denote $\mathbf{x}'_{i+1} \equiv \mathbf{x}'(\lambda_i + \Delta\lambda_i)$, $\Delta\mathbf{x}_{i+1} \equiv \mathbf{x}_{i+1} - \mathbf{x}_s(\lambda_{i+1})$, $\Delta\mathbf{x}'_{i+1} \equiv \mathbf{x}'_{i+1} - \mathbf{x}_s(\lambda_{i+1})$. Notice that $x_i = x'_i$. Consider the Taylor expansion

$$\mathbf{x}(\lambda + \Delta\lambda) = \sum_{j=0}^n \frac{1}{j!} \Delta\lambda^j \mathbf{x}^{(j)}(\lambda) + \mathcal{O}(\Delta\lambda^{n+1}). \quad (26)$$

Several equations follow from the Taylor expansion which will be of use:

$$\mathbf{x}'_{i+1} = \mathbf{x}_i + \sum_{j=1}^n \frac{1}{j!} \Delta\lambda^j \mathbf{x}^{(j)}(\lambda) + \mathcal{O}(\Delta\lambda^{n+1}), \quad (27)$$

$$\Delta\mathbf{x}'_{i+1} = \Delta\mathbf{x}_i + \sum_{j=1}^n \frac{1}{j!} \Delta\lambda^j \mathbf{x}^{(j)}(\lambda) + \mathcal{O}(\Delta\lambda^{n+1}), \quad (28)$$

$$\sum_{j=1}^n \frac{1}{j!} \Delta\lambda^j \mathbf{x}^{(j)}(\lambda) = \mathbf{x}'_{i+1} - \mathbf{x}_i + \mathcal{O}(\Delta\lambda^{n+1}). \quad (29)$$

Equation (29) can be used in equation (25) to obtain

$$\begin{aligned} \mathbf{x}_{i+1} &= \mathbf{x}_i - \gamma_i \Delta\lambda_i \mathcal{H}^*(\mathcal{H}(\mathbf{x}_i, \lambda_i), \lambda_i) + \mathbf{x}'_{i+1} - \mathbf{x}_i + \mathcal{O}(\Delta\lambda_i^{n+1}) \\ &\Rightarrow \mathbf{x}_{i+1} = \mathbf{x}'_{i+1} - \gamma_i \Delta\lambda_i \mathcal{H}^*(\mathcal{H}(\mathbf{x}_i, \lambda_i), \lambda_i) + \mathcal{O}(\Delta\lambda_i^{n+1}) \\ &\Rightarrow \Delta\mathbf{x}_{i+1} = \Delta\mathbf{x}'_{i+1} - \gamma_i \Delta\lambda_i \mathcal{H}^*(\mathcal{H}(\mathbf{x}_i, \lambda_i), \lambda_i) + \mathcal{O}(\Delta\lambda_i^{n+1}) \end{aligned} \quad (30)$$

Pre-multiplying both sides by its transpose, this becomes

$$\begin{aligned} \Rightarrow \Delta\mathbf{x}_{i+1}^T \Delta\mathbf{x}_{i+1} &= \Delta\mathbf{x}'_{i+1}^T \Delta\mathbf{x}'_{i+1} - 2\gamma_i \Delta\lambda_i \Delta\mathbf{x}'_{i+1}^T \mathcal{H}^*(\mathcal{H}(\mathbf{x}_i, \lambda_i), \lambda_i) \\ &\quad + \gamma_i^2 \Delta\lambda_i^2 [\mathcal{H}^*(\mathcal{H}(\mathbf{x}_i, \lambda_i), \lambda_i)]^T \mathcal{H}^*(\mathcal{H}(\mathbf{x}_i, \lambda_i), \lambda_i) + \mathcal{O}(\Delta\lambda_i^{n+1}). \end{aligned} \quad (31)$$

From the Taylor expansion (28), we see that

$$\begin{aligned} \gamma_i \Delta\lambda_i \Delta\mathbf{x}'_{i+1}^T &= \gamma_i \Delta\lambda_i (\Delta\mathbf{x}_i^T + \mathcal{O}(\Delta\lambda)) \\ &= \gamma_i \Delta\lambda_i \Delta\mathbf{x}_i^T + \mathcal{O}(\Delta\lambda^2). \end{aligned} \quad (32)$$

Substituting this into equation (31) gives

$$\begin{aligned} \Delta\mathbf{x}_{i+1}^T \Delta\mathbf{x}_{i+1} &= \Delta\mathbf{x}'_{i+1}^T \Delta\mathbf{x}'_{i+1} - 2\gamma_i \Delta\lambda_i \Delta\mathbf{x}_i^T \mathcal{H}^*(\mathcal{H}(\mathbf{x}_i, \lambda_i), \lambda_i) \\ &\quad + \gamma_i^2 \Delta\lambda_i^2 [\mathcal{H}^*(\mathcal{H}(\mathbf{x}_i, \lambda_i), \lambda_i)]^T \mathcal{H}^*(\mathcal{H}(\mathbf{x}_i, \lambda_i), \lambda_i) + \mathcal{O}(\Delta\lambda_i^2). \end{aligned} \quad (33)$$

To proceed, consider the Taylor expansions

$$\mathcal{H}(\mathbf{x}_i, \lambda_i) = \mathcal{H}(\mathbf{x}_s, \lambda_i) + \nabla_{\mathbf{x}} \mathcal{H}(\mathbf{x}_s, \lambda_i) \Delta \mathbf{x}_i + \mathcal{O}(\|\Delta \mathbf{x}_i\|^2), \quad (34)$$

$$\nabla \mathcal{H}(\mathbf{x}_s, \lambda_i) = \nabla_{\mathbf{x}} \mathcal{H}(\mathbf{x}_s + \Delta \mathbf{x}_i, \lambda_i) + \mathcal{O}(\|\Delta \mathbf{x}_i\|). \quad (35)$$

Since additionally $\mathcal{H}(\mathbf{x}_s, \lambda_i) = \mathbf{0}$,

$$\begin{aligned} & [\nabla \mathcal{H}(\mathbf{x}_i, \lambda_i)]^{-1} \mathcal{H}(\mathbf{x}_i, \lambda_i) = \Delta \mathbf{x}_i + \mathcal{O}(\|\Delta \mathbf{x}_i\|^2) \\ \Rightarrow & \left[[\nabla \mathcal{H}(\mathbf{x}_i, \lambda_i)]^{-1} \mathcal{H}(\mathbf{x}_i, \lambda_i) \right]^T [\nabla \mathcal{H}(\mathbf{x}_i, \lambda_i)]^{-1} \mathcal{H}(\mathbf{x}_i, \lambda_i) = \Delta \mathbf{x}_i^T \Delta \mathbf{x}_i + \mathcal{O}(\|\Delta \mathbf{x}_i\|^3), \end{aligned} \quad (36)$$

which can be used with equation (33) to get

$$\begin{aligned} \Delta \mathbf{x}_{i+1}^T \Delta \mathbf{x}_{i+1} = & \Delta \mathbf{x}'_{i+1}{}^T \Delta \mathbf{x}'_{i+1} - 2\gamma_i \Delta \lambda_i \Delta \mathbf{x}_i^T \mathcal{H}^*(\mathcal{H}(\mathbf{x}_i, \lambda_i), \lambda_i) + \gamma_i^2 \Delta \lambda_i^2 \Delta \mathbf{x}_i^T \Delta \mathbf{x}_i \\ & + \gamma_i^2 \Delta \lambda_i^2 \mathcal{O}(\|\Delta \mathbf{x}_i\|^3) + \mathcal{O}(\Delta \lambda_i^2). \end{aligned} \quad (37)$$

Recall the definition of the forward dynamic inverse (11). Applying Theorems 1 and 5 to equation (37) produces the inequality

$$\begin{aligned} \Delta \mathbf{x}_{i+1}^T \Delta \mathbf{x}_{i+1} & < \Delta \mathbf{x}_i^T \Delta \mathbf{x}_i + \varepsilon - 2\gamma_i \Delta \lambda_i \beta \Delta \mathbf{x}_i^T \Delta \mathbf{x}_i + \gamma_i^2 \Delta \lambda_i^2 \Delta \mathbf{x}_i^T \Delta \mathbf{x}_i + \gamma_i^2 \Delta \lambda_i^2 \mathcal{O}(\|\Delta \mathbf{x}_i\|^3) + \mathcal{O}(\Delta \lambda_i^2) \\ \Rightarrow & \Delta \mathbf{x}_{i+1}^T \Delta \mathbf{x}_{i+1} < \left(1 + \gamma_i^2 \Delta \lambda_i^2 - 2\gamma_i \Delta \lambda_i \beta\right) \Delta \mathbf{x}_i^T \Delta \mathbf{x}_i + \varepsilon + \gamma_i^2 \Delta \lambda_i^2 \mathcal{O}(\|\Delta \mathbf{x}_i\|^3) + \mathcal{O}(\Delta \lambda_i^2). \end{aligned} \quad (38)$$

It is ensured by Theorem 4 that there exist r , $\Delta \lambda_i$, and $0 < \beta < \frac{1}{\gamma_i \Delta \lambda_i}$ such that

$$\gamma_i^2 \Delta \lambda_i^2 \mathcal{O}(\|\Delta \mathbf{x}_i\|^3) + \mathcal{O}(\Delta \lambda_i^2) + \varepsilon < \beta (1 - \gamma_i \Delta \lambda_i \beta) \Delta \mathbf{x}_i^T \Delta \mathbf{x}_i. \quad (39)$$

Fixing $k \equiv \gamma_i \Delta \lambda_i$, $k \in \mathbb{R}$, $k \leq 1$ for all i and using the inequality (39) with equation (38) gives

$$\begin{aligned} \Delta \mathbf{x}_{i+1}^T \Delta \mathbf{x}_{i+1} & < (2 - 2k\beta) \Delta \mathbf{x}_i^T \Delta \mathbf{x}_i + \beta (1 - k\beta) \Delta \mathbf{x}_i^T \Delta \mathbf{x}_i \\ \Rightarrow & \Delta \mathbf{x}_{i+1}^T \Delta \mathbf{x}_{i+1} < (2 + \beta) (1 - k\beta) \Delta \mathbf{x}_i^T \Delta \mathbf{x}_i. \end{aligned} \quad (40)$$

The error is thus decreasing if

$$(2 + \beta) (1 - k\beta) < 1, \quad (41)$$

which leads to the condition

$$\frac{1}{2k} - 1 + \sqrt{1 + \frac{1}{4k^2}} < \beta < \frac{1}{k}. \quad (42)$$

Recall, viz. Theorem 4, that when the nearby inverse Jacobian is used as the dynamic inverse the convergence parameter satisfies $0 < \beta < 1$. Under this condition, it is additionally necessary that

$$\frac{2}{3} \leq k \leq 1. \quad (43)$$

In the special case of $k = 1$, the constraint on β is

$$\frac{\sqrt{5} - 1}{2} < \beta < 1. \quad (44)$$

□

Remark 4. Theorem 6 also establishes convergence for the original monolithic homotopy continuation algorithm for the special case of $\gamma_i \Delta \lambda_i = 1$. Previously [6], we had only managed to establish convergence for sufficiently small $\gamma_i \Delta \lambda_i$ and had inferred convergence of the $\gamma_i \Delta \lambda_i = 1$ case based on comparison to the predictor-corrector algorithm.

Remark 5. The sufficient conditions for convergence (42) and (43) pose some additional restriction on the minimum radius required for the dynamic inverse, vis. Definition 1, and the minimum allowable relaxation factor $\gamma_i \Delta \lambda_i$. However, many inequalities were imposed in the proof which we expect drove the lower limits of both values up higher than necessary. Future work may be targeted at attempting to adjust the proof to achieve less restrictive bounds on β and $\gamma_i \Delta \lambda_i$.

Remark 6. In equation (33), high order of accuracy was lost due to the use of a second order dynamic inverse. In fact, expanding $\Delta \mathbf{x}_i^T \Delta \mathbf{x}_i$ in a Taylor expansion indicates that ε is actually $\mathcal{O}(\Delta \lambda_i)$, so higher order accuracy is lost regardless of the order of both the dynamic inverse and the predictor. Being limited to first order accuracy is however not crucial since the limiting case of $\Delta \lambda \rightarrow 0$ is of little to no practical interest and we have already shown previously that higher order predictors can be more accurate than lower order ones for practical values of $\Delta \lambda$ [5].

Similarly, convergence is established for the reverse-mode algorithm and is formalized in the following theorem.

Theorem 7. Let $\mathbf{x}_s(\lambda)$ be a continuous isolated solution of a regular homotopy $\mathcal{H}(\mathbf{x}, \lambda) = \mathbf{0}$, $\mathcal{H} : \mathbb{R}^N \times \mathbb{R} \rightarrow \mathbb{R}^N$. Assume that $\mathcal{H}(\mathbf{x}, \lambda)$ is C^∞ in both \mathbf{x} and λ . Let $\mathcal{H}^*(\mathbf{w}, \lambda) = -[\nabla_{\mathbf{x}} \mathcal{H}(\mathbf{x}, \lambda)]^{-1} \mathbf{w}$ be a reverse-mode dynamic inverse of $\mathcal{H}(\mathbf{x}, \lambda)$ on $\mathcal{B}_r(\mathbf{x}_s(\lambda))$. Then for sufficiently large $\Delta \lambda_i \equiv \lambda_{i+1} - \lambda_i < 0$ and for any $-1 < \gamma_i \Delta \lambda_i \leq -\frac{2}{3}$ there exists $\mathcal{B}_r(\mathbf{x}_s(\lambda))$ such that the difference equation

$$\mathbf{x}_{i+1} = \mathbf{x}_i - \gamma_i \Delta \lambda_i \mathcal{H}^*(\mathcal{H}(\mathbf{x}_i, \lambda_i), \lambda_i) + \sum_{k=1}^n \frac{1}{k!} \Delta \lambda_i^k \mathbf{x}^{(k)}(\lambda_i) \quad (45)$$

converges to $\mathbf{x}_s(\lambda)$ for any $n \geq 1$, where the bracketed superscript indicates differentiation.

Proof. The proof is identical to the proof of Theorem 6 until equation (37). Applying Theorems 2 and 5 to equation (37) produces the inequality

$$\begin{aligned} \Delta \mathbf{x}_{i+1}^T \Delta \mathbf{x}_{i+1} &< \Delta \mathbf{x}_i^T \Delta \mathbf{x}_i + \varepsilon + 2\gamma_i \Delta \lambda_i \beta \Delta \mathbf{x}_i^T \Delta \mathbf{x}_i + \gamma_i^2 \Delta \lambda_i^2 \Delta \mathbf{x}_i^T \Delta \mathbf{x}_i + \gamma_i^2 \Delta \lambda_i^2 \mathcal{O}(\|\Delta \mathbf{x}_i\|^3) + \mathcal{O}(\Delta \lambda_i^2) \\ &\Rightarrow \Delta \mathbf{x}_{i+1}^T \Delta \mathbf{x}_{i+1} < (1 + \gamma_i^2 \Delta \lambda_i^2 + 2\gamma_i \Delta \lambda_i \beta) \Delta \mathbf{x}_i^T \Delta \mathbf{x}_i + \varepsilon + \gamma_i^2 \Delta \lambda_i^2 \mathcal{O}(\|\Delta \mathbf{x}_i\|^3) + \mathcal{O}(\Delta \lambda_i^2). \end{aligned} \quad (46)$$

It is ensured by Theorem 5 that there exist r , $\Delta \lambda_i$, and $0 < \beta < -\frac{1}{\gamma_i \Delta \lambda_i}$ such that

$$\gamma_i^2 \Delta \lambda_i^2 \mathcal{O}(\|\Delta \mathbf{x}_i\|^3) + \mathcal{O}(\Delta \lambda_i^2) + \varepsilon < \beta (1 + \gamma_i \Delta \lambda_i \beta) \Delta \mathbf{x}_i^T \Delta \mathbf{x}_i. \quad (47)$$

Fixing $k \equiv -\gamma_i \Delta \lambda_i$, $k \in \mathbb{R}$, $k \leq 1$ for all i and using the inequality (47) with equation (46) gives

$$\begin{aligned} \Delta \mathbf{x}_{i+1}^T \Delta \mathbf{x}_{i+1} &< (2 - 2k\beta) \Delta \mathbf{x}_i^T \Delta \mathbf{x}_i + \beta (1 - k\beta) \Delta \mathbf{x}_i^T \Delta \mathbf{x}_i \\ &\Rightarrow \Delta \mathbf{x}_{i+1}^T \Delta \mathbf{x}_{i+1} < (2 + \beta) (1 - k\beta) \Delta \mathbf{x}_i^T \Delta \mathbf{x}_i, \end{aligned} \quad (48)$$

thus proving convergence under identical conditions as Theorem 6. \square

Finally, convergence is established for any general parametrization. First, a more general version of Theorem 5 is needed.

Theorem 8. *Let the solution pair $\mathbf{x}_s(s), \lambda(s)$ be a continuous isolated solution to $\mathcal{H}(\mathbf{x}, \lambda) = \mathbf{0}$, $\mathcal{H} : \mathbb{R}^N \times \mathbb{R} \rightarrow \mathbb{R}^N$. Let the solution pair $\mathbf{x}'_s(s), \lambda(s)$ satisfy*

$$\mathcal{H}'(\mathbf{x}, \lambda) \equiv \mathcal{H}(\mathbf{x}, \lambda) - \mathcal{K} = \mathbf{0}, \quad (49)$$

where $\mathcal{K} : \mathbb{R}^N \rightarrow \mathbb{R}^N$, $\mathcal{K} = \mathcal{H}(\mathbf{x}_0, \lambda_0)$ for some fixed $\mathbf{x}_0 \in \mathbb{R}^N$, $\lambda_0 \in \mathbb{R}$, $0 < \lambda_0 < 1$. Assume that $\mathcal{H} : \mathbb{R}^N \times \mathbb{R} \rightarrow \mathbb{R}^N$ is continuous with nonsingular Jacobian along $\mathbf{x}_s(s)$ and $\mathbf{x}'_s(s)$. Define $\Delta \mathbf{x} \equiv \mathbf{x}'_s(s) - \mathbf{x}_s(s)$ and let $\varepsilon \in \mathbb{R}$, $\delta \in \mathbb{R}$. Then $\forall \varepsilon > 0$, $\exists \delta > 0$ such that

$$|\Delta \mathbf{x}(s + \delta)^T \Delta \mathbf{x}(s + \delta) - \Delta \mathbf{x}(s)^T \Delta \mathbf{x}(s)| < \varepsilon. \quad (50)$$

Proof. This is analogous to the proof of Theorem 5, replacing $\mathbf{x}(\lambda)$ with $c(s)$. \square

We now state our convergence result for the most general case.

Theorem 9. *Let the solution pair $\mathbf{x}_s(s), \lambda(s)$ be a continuous isolated solution of a regular homotopy $\mathcal{H}(\mathbf{x}, \lambda) = \mathbf{0}$, $\mathcal{H} : \mathbb{R}^N \times \mathbb{R} \rightarrow \mathbb{R}^N$. Assume that $\mathcal{H}(\mathbf{x}, \lambda)$ is C^∞ in both \mathbf{x} and λ . Let $\mathcal{H}^*(\mathbf{w}, \lambda) = [\nabla_{\mathbf{x}} \mathcal{H}(\mathbf{x}, \lambda)]^{-1} \mathbf{w}$ be a forward dynamic inverse of $\mathcal{H}(\mathbf{x}, \lambda)$ on $\mathcal{B}_r(\mathbf{x}_s(s))$. Then for sufficiently small $\Delta s_i \equiv s_{i+1} - s_i > 0$ and for any $\frac{2}{3} < \gamma_i \Delta s_i \leq 1$ there exists $\mathcal{B}_r(\mathbf{x}_s(s))$ such that the difference equation*

$$\mathbf{x}_{i+1} = \mathbf{x}_i - \gamma_i \Delta s_i \mathcal{H}^*(\mathcal{H}(\mathbf{x}_i, \lambda_i), \lambda_i) + \sum_{k=1}^n \frac{1}{k!} \Delta s_i^k \mathbf{x}^{(k)}(\lambda_i) \quad (51)$$

converges to $\mathbf{x}_s(s)$ for any $n \geq 1$, where the bracketed superscript indicates differentiation.

Proof. Consider the Taylor expansion

$$\mathbf{x}(s + \Delta s) = \sum_{j=0}^n \frac{1}{j!} \Delta s^j \mathbf{x}^{(j)}(s) + \mathcal{O}(\Delta s^{n+1}). \quad (52)$$

Let $\mathbf{x}'_s(s)$ be the (presumably) continuous solution to

$$\mathcal{H}'(\mathbf{x}, \lambda) = \mathcal{H}(\mathbf{x}, \lambda) - \mathcal{H}(\mathbf{x}_i, \lambda_i) = \mathbf{0}. \quad (53)$$

Denote $\mathbf{x}'_{i+1} \equiv \mathbf{x}'_s(s_i + \Delta s_i)$. Then equation (51) can be written as

$$\mathbf{x}_{i+1} = \mathbf{x}_i - \gamma_i \Delta s_i \mathcal{H}^*(\mathcal{H}(\mathbf{x}_i, \lambda_i), \lambda_i) + \mathbf{x}'_{i+1} - \mathbf{x}'_s(s_i) + \mathcal{O}(\Delta s_i^{n+1}). \quad (54)$$

Further denote $\Delta \mathbf{x}_{i+1} \equiv \mathbf{x}_{i+1} - \mathbf{x}_s(s_{i+1})$, $\Delta \mathbf{x}'_{i+1} \equiv \mathbf{x}'_{i+1} - \mathbf{x}_s(s_{i+1})$. Since $\mathbf{x}'_s(s_i) = \mathbf{x}_i$, equation (54) becomes

$$\begin{aligned} \mathbf{x}_{i+1} &= \mathbf{x}'_{i+1} - \gamma_i \Delta s_i \mathcal{H}^*(\mathcal{H}(\mathbf{x}_i, \lambda_i), \lambda_i) + \mathcal{O}(\Delta s_i^{n+1}) \\ &\Rightarrow \Delta \mathbf{x}_{i+1} = \Delta \mathbf{x}'_{i+1} - \gamma_i \Delta s_i \mathcal{H}^*(\mathcal{H}(\mathbf{x}_i, \lambda_i), \lambda_i) + \mathcal{O}(\Delta s_i^{n+1}) \\ &\Rightarrow \Delta \mathbf{x}_{i+1}^T \Delta \mathbf{x}_{i+1} = \Delta \mathbf{x}'_{i+1}^T \Delta \mathbf{x}'_{i+1} - 2\gamma_i \Delta s_i \Delta \mathbf{x}'_{i+1}^T \mathcal{H}^*(\mathcal{H}(\mathbf{x}_i, \lambda_i), \lambda_i) \\ &\quad + \gamma_i^2 \Delta s_i^2 [\mathcal{H}^*(\mathcal{H}(\mathbf{x}_i, \lambda_i), \lambda_i)]^T \mathcal{H}^*(\mathcal{H}(\mathbf{x}_i, \lambda_i), \lambda_i) + \mathcal{O}(\Delta s_i^{n+1}). \end{aligned} \quad (55)$$

From this point forward, the proof is identical to the proof of Theorem 6 with the following modifications: $\Delta \lambda$ is replaced with Δs in all occurrences, and the reference to Theorem 5 is replaced with a reference to Theorem 8. \square

Remark 7. An estimate of $\lambda(s_{i+1})$ can be obtained using the Taylor expansion

$$\lambda(s_i + \Delta s_i) = \sum_{j=0}^n \frac{1}{j!} \Delta s_i^j \lambda^{(j)}(s_i). \quad (56)$$

Remark 8. Theorem 6 follows from Theorem 9 using the parametrization $\dot{\lambda}(s) = 1$. Theorem 7 follows from Theorem 9 using the parametrization $\dot{\lambda}(s) = -1$.

7. Differentiation of Implicitly-Defined Curves

We have recently studied techniques for the efficient differentiation of implicitly-defined curves [5], extending the work of Refs. [24, 28, 31, 33] for efficient application to sparse systems of equations. In this section, define the curve $c(s) \in \mathbb{R}^{N+1}$:

$$c(s) \equiv (\mathbf{x}(s); \lambda(s)). \quad (57)$$

7.1. n -th Curve Derivative with Arc-Length Parametrization

The derivation is provided by Brown and Zingg [5]. The first derivative pair $\dot{\mathbf{x}}(s)$ and $\dot{\lambda}(s)$ is given by

$$\dot{\mathbf{x}} = -\dot{\lambda} \mathbf{z} \quad (58)$$

$$\dot{\lambda} = \frac{-1}{\sqrt{\mathbf{z} \cdot \mathbf{z} + 1}}, \quad (59)$$

where \mathbf{z} is obtained by solving

$$\nabla_{\mathbf{x}} \mathcal{H}(c(s)) \mathbf{z} = \frac{\partial}{\partial \lambda} \mathcal{H}(c(s)). \quad (60)$$

The n th derivative is calculated from the $n - 1$ st derivative using the equation

$$\mathbf{x}^{(n)} = \mathbf{z}_n - \lambda^{(n)} \mathbf{z}, \quad (61)$$

where \mathbf{z}_n is obtained by solving

$$\nabla_{\mathbf{x}} \mathcal{H}(c(s)) \mathbf{z}_n = -\mathbf{w}_n \quad (62)$$

and \mathbf{w}_n is computed from

$$\mathbf{w}_n \equiv \sum \left\{ \frac{n!}{\prod_{j=1}^n j!^{m_j} m_j!} \nabla^{\sum_{j=1}^n m_j} \mathcal{H}(c(s)) \prod_{j=1}^n [c^{(j)}(s)]^{m_j} \right\} - \nabla \mathcal{H}(c(s)) c^{(n)}(s), \quad (63)$$

where the outer summation is taken over all n -tuples of non-negative integers $\{m_1, \dots, m_n\}$ such that

$$\sum_{j=1}^n j m_j = n \quad (64)$$

and the notation which seems to indicate the product $[c^{(j)}(s)]^{m_j}$ for all j is intended to indicate that $c^{(j)}(s)$ appears with multiplicity m_j as input to $\nabla^{\sum_{j=1}^n m_j} \mathcal{H}(c(s))$. Furthermore, $\lambda^{(n)}$ is computed directly from

$$\lambda^{(n)} = \frac{\mathbf{z}_n \cdot \dot{\mathbf{x}} - c^{(n)} \cdot \dot{c}}{\sqrt{\mathbf{z} \cdot \mathbf{z} + 1}}, \quad (65)$$

where

$$c^{(n)} \cdot \dot{c} = \begin{cases} -\sum_{k=1}^{\frac{n-3}{2}} \binom{n-1}{k} c^{(k+1)} \cdot c^{(n-k)} - \frac{1}{2} \binom{n-1}{\frac{n-1}{2}} c^{((n+1)/2)} \cdot c^{((n+1)/2)} & n \text{ is odd} \\ -\sum_{k=1}^{\frac{n}{2}-1} \binom{n-1}{k} c^{(k+1)} \cdot c^{(n-k)} & n \text{ is even} \end{cases} \quad (66)$$

is also a direct calculation.

7.2. n -th Curve Derivative with Parametrization $\lambda(s) = -1$

The derivation is provided by Brown and Zingg [5]. The first derivative pair is given by

$$\dot{\mathbf{x}} = \mathbf{z} \quad (67)$$

$$\dot{\lambda} = -1, \quad (68)$$

where \mathbf{z} is again given by solving the linear system in equation (60). The n th derivative is calculated from the $n - 1$ st derivative using the equation

$$\nabla_{\mathbf{x}} \mathcal{H}(c(s)) \mathbf{x}^{(n)}(s) = -\mathbf{w}'_n, \quad (69)$$

$$\mathbf{w}'_n = \frac{d}{ds} \mathcal{H}(c(s)) - \nabla \mathcal{H}(c(s)) \mathbf{x}^{(n)}(s), \quad (70)$$

$\mathbf{w}'_n \in \mathbb{R}^N$, where the prime distinguishes \mathbf{w}'_n from \mathbf{w}_n and $\frac{d}{ds} \mathcal{H}(c(s))$ is again calculated from equation (63). By equation (68),

$$\lambda^{(k)}(s) = 0 \quad (71)$$

for all $k > 1$.

7.3. Tensor-Vector Product Estimation

The current method used to approximate the tensor-vector products is to use a finite-differencing approach. While practical and inexpensive, it has been found that this estimate is not always accurate, and is especially unreliable for larger or more complex cases [5]. As the need to estimate tensor-vector products for large sparse systems of equations is seldom a problem of practical significance, this is a problem which has yet to be thoroughly explored.

While automatic differentiation [2] may be an option, this would add significant overhead cost to the primal equations. The complex step method [23, 32] is a useful way to accurately approximate first derivatives but for higher derivatives it provides no advantage over ordinary finite-differencing. Using higher precision is of course possible but is too computationally expensive [5]. A possible solution may be to use hyper-dual numbers [11] or hyper-complex numbers. To our knowledge, this has yet to be investigated due to lack of applications prior to this paper.

8. Practical Application of the Algorithm

Brown and Zingg [4, 6] developed the monolithic homotopy continuation algorithm in part for the efficiency gains in being able to combine the linear solves required in the predictor and corrector stages of the algorithm. This linear solve gives an update including both a predictor and corrector component. However, the tangent calculation cannot be combined with the corrector if higher degree curve derivatives are needed because the tangent itself is needed in subsequent derivative evaluations. Since the tangent vector is needed for the higher derivative calculations, the corrector (dynamic inverse) and tangent calculations should be separated into two linear solves. However, we will see in this section that it can still be possible to combine the linear solve for the corrector with the linear solve needed for the n th curve derivative calculation.

8.1. Arc-Length Parametrization

The algorithm is applied using equation (51). The first derivative pair is calculated using equations (58) and (59), and each consecutive derivative up to order $n - 1$ is calculated from equation (61). Let

$$S_{n-1} = \sum_{k=1}^{n-1} \frac{1}{k!} \Delta s_i^k \mathbf{x}^{(k)}(s_i). \quad (72)$$

Then

$$\begin{aligned} \mathbf{x}_{i+1} &= \mathbf{x}_i - \gamma_i \Delta s_i [\nabla_{\mathbf{x}} \mathcal{H}(\mathbf{x}_i, \lambda_i)]^{-1} \mathcal{H}(\mathbf{x}_i, \lambda_i) + \frac{1}{n!} \Delta s_i^n \mathbf{x}^{(n)}(s_i) + S_{n-1} \\ &= \mathbf{x}_i - \gamma_i \Delta s_i [\nabla_{\mathbf{x}} \mathcal{H}(\mathbf{x}_i, \lambda_i)]^{-1} \mathcal{H}(\mathbf{x}_i, \lambda_i) + \frac{1}{n!} \Delta s_i^n (\mathbf{z}_n - \lambda^{(n)} \mathbf{z}) + S_{n-1} \\ &= \mathbf{x}_i - \gamma_i \Delta s_i [\nabla_{\mathbf{x}} \mathcal{H}(\mathbf{x}_i, \lambda_i)]^{-1} \mathcal{H}(\mathbf{x}_i, \lambda_i) - \frac{1}{n!} \Delta s_i^n [\nabla_{\mathbf{x}} \mathcal{H}(\mathbf{x}_i, \lambda_i)]^{-1} \mathbf{w}_n \\ &\quad + \frac{\Delta s_i^n}{n! \sqrt{\mathbf{z} \cdot \mathbf{z} + 1}} [\mathbf{z}_n \cdot \dot{\mathbf{x}}_i - c^{(n)} \cdot \dot{c}] \mathbf{z} + S_{n-1} \\ &= \mathbf{x}_i - [\nabla_{\mathbf{x}} \mathcal{H}(\mathbf{x}_i, \lambda_i)]^{-1} \left[\gamma_i \Delta s_i \mathcal{H}(\mathbf{x}_i, \lambda_i) - \frac{1}{n!} \Delta s_i^n \mathbf{w}_n \right] \\ &\quad - \frac{\Delta s_i^n}{n! \sqrt{\mathbf{z} \cdot \mathbf{z} + 1}} \left[([\nabla_{\mathbf{x}} \mathcal{H}(\mathbf{x}_i, \lambda_i)]^{-1} \mathbf{w}_n) \cdot \dot{\mathbf{x}} + c^{(n)} \cdot \dot{c} \right] \mathbf{z} + S_{n-1}, \end{aligned} \quad (73)$$

where $c^{(n)} \cdot \dot{c}$ can be evaluated using equation (66).

8.2. $\dot{\lambda}(s) = -1$ Parametrization

The algorithm is applied using equation (51). The first derivative pair is calculated using equations (67) and (68), and each consecutive derivative up to order $n - 1$ is calculated from equation (69). Let

$$S_{n-1} = \sum_{k=1}^{n-1} \frac{1}{k!} \Delta s_i^k \mathbf{x}^{(k)}(s_i). \quad (74)$$

Then

$$\begin{aligned}
\mathbf{x}_{i+1} &= \mathbf{x}_i - \gamma_i \Delta s_i [\nabla_{\mathbf{x}} \mathcal{H}(\mathbf{x}_i, \lambda_i)]^{-1} \mathcal{H}(\mathbf{x}_i, \lambda_i) + \frac{1}{n!} \Delta s_i^n \mathbf{x}_i^{(n)}(s_i) + S_{n-1} \\
&= \mathbf{x}_i - \gamma_i \Delta s_i [\nabla_{\mathbf{x}} \mathcal{H}(\mathbf{x}_i, \lambda_i)]^{-1} \mathcal{H}(\mathbf{x}_i, \lambda_i) - \frac{1}{n!} \Delta s_i^n [\nabla_{\mathbf{x}} \mathcal{H}(c(s))]^{-1} \mathbf{w}'_n + S_{n-1} \\
&= \mathbf{x}_i - [\nabla_{\mathbf{x}} \mathcal{H}(\mathbf{x}_i, \lambda_i)]^{-1} \left(\gamma_i \Delta s_i \mathcal{H}(\mathbf{x}_i, \lambda_i) + \frac{1}{n!} \Delta s_i^n \mathbf{w}'_n \right) + S_{n-1}
\end{aligned} \tag{75}$$

where $c^{(n)} \cdot \dot{c}$ can be evaluated using equation (66).

8.3. The Monolithic Homotopy Continuation Algorithm with Degree n Derivative

A high-level pseudo-code for the calculation is summarized in Algorithm 2, which can be compared to the original algorithm shown as Algorithm 1.

Algorithm 1: Original Monolithic homotopy continuation algorithm

```

Set  $\lambda = 1$  and solve  $\mathcal{G}(\mathbf{x}) = \mathbf{0}$  if necessary
while  $\lambda > 0$  do
  Get  $\gamma, \mathcal{H}, \|\mathcal{H}\|$ , and  $-\gamma\mathcal{H} + \mathcal{G} - \mathcal{R}$ 
  Form and factor the preconditioner approximating the matrix  $\nabla_{\mathbf{x}} \mathcal{H}$ 
  Solve the linear system  $\nabla_{\mathbf{x}} \mathcal{H} \Delta \mathbf{x} = [-\gamma\mathcal{H} + \mathcal{G} - \mathcal{R}]$  for  $\Delta \mathbf{x}$ 
  Choose  $\Delta s$ 
  Update  $\lambda$  and  $\mathbf{x}$ 
end

```

Algorithm 2: Monolithic homotopy continuation algorithm including derivatives up to degree n

```

Set  $\lambda = 1$  and solve  $\mathcal{G}(\mathbf{x}) = \mathbf{0}$  if necessary
while  $\lambda > 0$  do
  Get  $\gamma, \mathcal{G}, \mathcal{R}, \mathcal{H}$ , and  $\|\mathcal{H}\|$ 
  Form and factor the preconditioner approximating the matrix  $\nabla_{\mathbf{x}} \mathcal{H}$ 
  for  $i = 0 : n - 1$  do
    Form  $\mathbf{w}_i$  and calculate  $\mathbf{x}^{(i)}$  based on Section 7.1 or 7.2
  end
  Choose  $\Delta s$ 
  Calculate  $\mathbf{w}_n$  and the combined final stage of the update based on Section 8.1 or 8.2.
  Update  $\lambda$  and  $\mathbf{x}$ 
end

```

8.4. Choice of Parametrization Based on the Analysis

We see from equations (73) and (75) that the calculation requires an additional linear solve when using an arclength parametrization because the inverse Jacobian appears in the inner product in equation (73) and cannot be factored out. This constitutes considerable extra cost which

we do not anticipate can be recovered by any benefits from potentially superior step-length adaptation capabilities. Hence, we choose to take the $\lambda(s) = -1$ parametrization approach through the rest of this study.

To perform one step of the algorithm using the n th derivative, $n - 1$ linear systems must be solved. Each of these linear systems has the same left-hand side but a different right-hand side. Currently, the approach taken is to use ILU(p)-preconditioned GMRES, where the ILU factorization is performed only once per iteration of the algorithm (e.g. once for each value of λ).

Since $\Delta\lambda$ is built into the sum S_{n-1} , step-length adaptation, if applied, must be performed prior to forming S_{n-1} . It is, however, possible to calculate each curve derivative vector prior to selecting $\Delta\lambda$. We propose adapting $\Delta\lambda$ to attempt to achieve consistent $\|S_{n-1}\|$, recognizing that S_{n-1} is the predictor-component of the update up to the $n - 1$ st term. As with our previous work with the original monolithic homotopy continuation algorithm [6], the target value of S_{n-1} can be based on the first iteration. We do not however investigate this approach in this paper as we are deferring comprehensive performance studies until the tensor-vector product accuracy issue is resolved.

9. Results

Since the accuracy of the finite-differencing method used to form the tensor-vector products can be unreliable, particularly for larger cases and especially for higher derivatives [5], we restrict the study to inviscid subsonic flow over the NACA 0012 geometry. Though this is a practical test case of scientific interest, it is far smaller and easier than the test cases that we are ultimately interested in and which have motivated the development of the new algorithm, and so we regard these results as preliminary.

9.1. Governing Equations

The test cases presented in this paper are all inviscid external compressible aerodynamic flows. The discretized Euler equations which are being solved for these test cases are given, for example, by Hicken and Zingg [16]. In this context, the state vector \mathbf{x} consists of four variables per node. For node index i :

$$\mathbf{x}_{[i]} = \begin{bmatrix} \rho_i \\ \rho_i u_i \\ \rho_i v_i \\ e_i \end{bmatrix}, \quad (76)$$

where ρ is the air density, u and v are Cartesian velocity components, and e is the energy, which, under the ideal gas assumption, is related to pressure p and velocities u and v through the formula

$$p = (\gamma_a - 1) \left(e - \frac{1}{2} \rho (u^2 + v^2) \right), \quad (77)$$

where $\gamma_a \in \mathbb{R}$ is the heat capacity ratio for air and is taken as 1.4.

9.2. Geometry

The NACA 0012 geometry is a well-known two-dimensional airfoil geometry often used for CFD testing and benchmarking and for which a large amount of experimental data exists. See McCroskey [25] for a summary and assessment of experimental data collected for this geometry prior to 1987. The grid used to represent the region surrounding the NACA 0012 airfoil in our study has an H topology and consists of 15390 nodes divided evenly into 18 blocks for parallelization on 18 processors. The Mach number is 0.3 and the angle of attack is 1° . Detailed accuracy studies on the derivative calculation have previously been performed for this test case by Brown and Zingg [5].

9.3. Accuracy Study

The purpose of this study is to develop a comparison between the augmented monolithic homotopy continuation algorithm and the original algorithm. Since no step-length adaptation is applied, $\Delta\lambda$ is maintained constant for each test case. Setting the finite-difference step size to $\delta = 10^{-12}$ in the tensor-vector product estimates (see Brown and Zingg [5]) was found to be fairly optimal for the $n = 2$ case but changing this value to $\delta = 10^{-8}$ affected the predicted residual by around 25%, performing better in some areas and worse in others, indicating that the error in the estimate remains significant.

The residual $\|H(\mathbf{x}, \lambda)\|$ gives an indication of curve-tracing accuracy and is recorded as a function of λ for several applications of the algorithm based on equation (75) with different values of n , where n is the degree of the Taylor polynomial used to build the predictor, viz. equation (25). The effect of the linear solver tolerance on the accuracy of the update is also investigated by comparing plots of $\|H(\mathbf{x}, \lambda)\|$ as a function of λ for $\tau_1 = 10^{-4}$ and $\tau_1 = 10^{-2}$, where τ_1 is the linear solver tolerance as it appears in equation (4). The value $\tau_1 = 10^{-4}$ is expected, based on experience, to give a very accurate update, whereas $\tau_1 = 10^{-2}$ is a value more typical of what we have typically used in practice [6, 16] as over-solving the linear system is computationally inefficient.

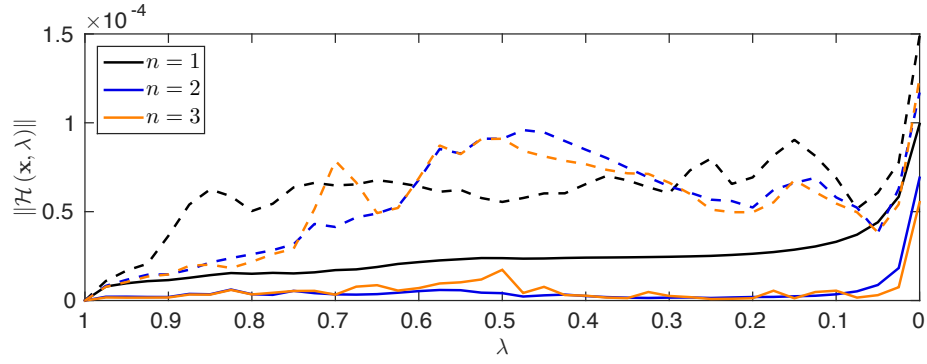
The residual history is presented in Figure 1. It can be seen that when the linear system is solved accurately, the $n = 2$ algorithm predicts the curve significantly more accurately than the $n = 1$ algorithm. From Figure 1a, this advantage can clearly be lost if the linear solver tolerance is relaxed, highlighting the importance of accurately forming the higher derivatives.

It seems apparent from Figure 1a that there is no benefit to augmenting the algorithm to $n = 3$. However, we suspect that this is due to inaccuracy in forming the tensor-vector products for this case. This is supported by our previous studies of the accuracy of the $n = 3$ derivative calculation for this case [5], where we found that the error could be on the order of 30% at some values of λ . We thus regard these results as inconclusive and the $n = 3$ option is thus omitted from further studies in this paper.

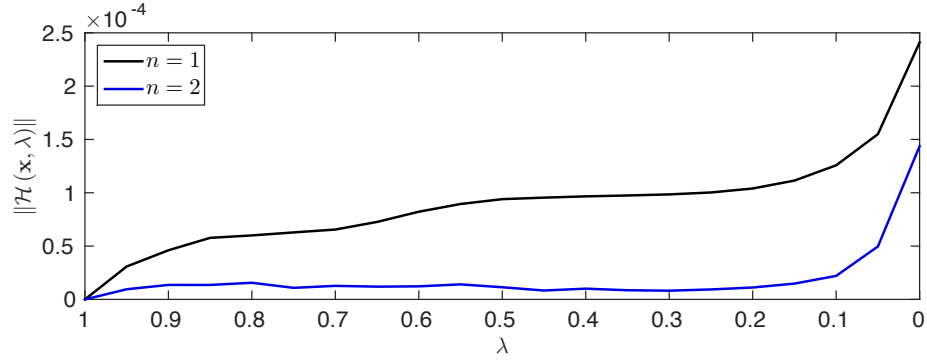
9.4. Preliminary Efficiency Study

Since the tensor-vector product accuracy issue has yet to be solved, the results in this study should be regarded as preliminary.

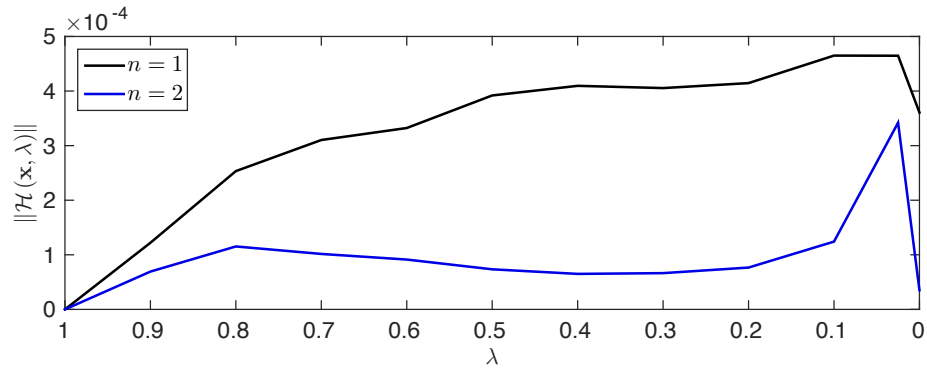
Since the continuation algorithm based on the second derivative requires twice as many linear solves as the $n = 1$ algorithm, and the linear solver is normally at least 90% of the cost for our applications, we assume that the algorithm is approximately twice as expensive per iteration. Hence, traversing can be obtained in approximately the same CPU time for the $n = 2$ case if the



(a) $|\Delta\lambda| = 0.025$; the solid and dashed lines correspond to $\tau_1 = 10^{-4}$ and 10^{-2} respectively



(b) $|\Delta\lambda| = 0.05$, $\tau_1 = 10^{-4}$



(c) $|\Delta\lambda| = 0.1$, $\tau_1 = 10^{-4}$

Figure 1: Comparison of continuation algorithms based on the n th derivative

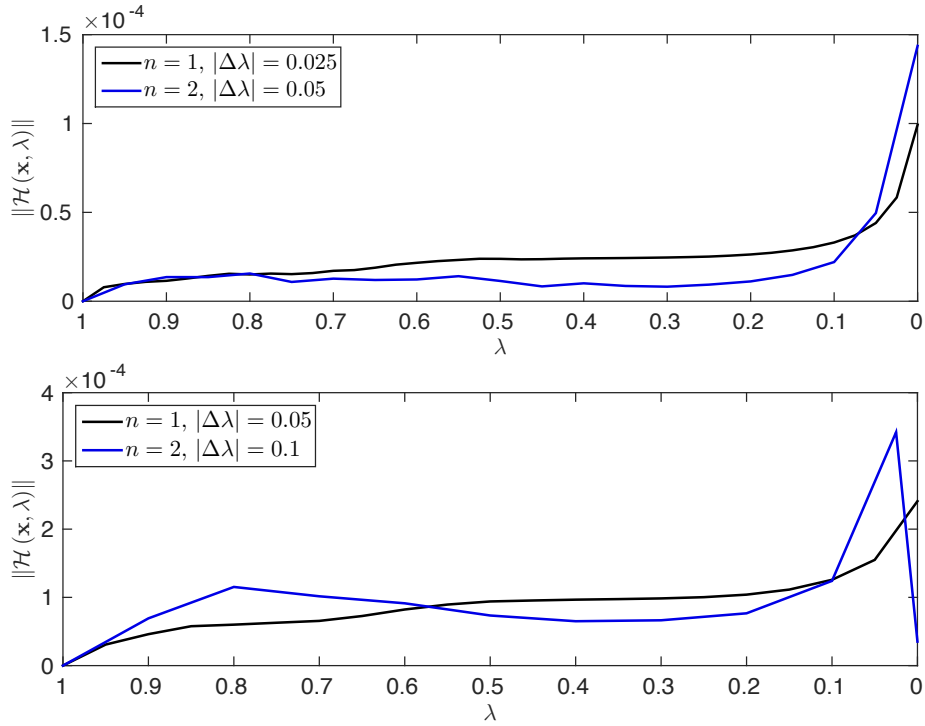


Figure 2: Cost-equal comparison of continuation algorithms based on the n th derivative with $\tau_1 = 10^{-4}$

step size is doubled. To get an idea of how the relative efficiency of the $n = 2$ algorithm compares to the $n = 1$ algorithm, we compare the accuracy of the two algorithms using double the step size for the $n = 2$ algorithm.

Two comparisons are shown in Figure 2. From the figures, it appears that similar curve tracing accuracy can be achieved in either case, indicating no clear gain or loss in efficiency. It is our expectation that these results will improve when the accuracy of the tensor-vector product estimate is improved.

9.5. Assessment

The results of Section 9.4 are actually very promising. Due to the considerable extra cost in forming the higher derivatives, it was not expected that the efficiency of the original algorithm could be surpassed, and perhaps doubtful if it could even be matched. As stated in the introduction, the primary motivation for developing this algorithm class was for the potential robustness gains in being able to better predict the curve. While such benefits are not apparent from this simple test case, they are anticipated for some cases which have proved challenging for the original algorithm [6] and so this study has certainly motivated further work in developing these methods.

10. Conclusions

The contributions of this work are the formulation, analysis, and numerical study of incorporating higher-order accurate predictors into the monolithic homotopy continuation algorithm. Some important analytical results concerning convergence of the algorithm were established, including convergence for $0 \leq |\gamma\Delta\lambda| \leq 1$ (Remark 4) and that the overall order of accuracy may be limited to first order regardless of the order of accuracy of the predictor (Remark 6). These results also contribute to our understanding of the original monolithic homotopy continuation algorithm as they had previously not been established.

While forming the update based on data near to the curve, as opposed to directly lying on the curve, ultimately restricts the order of accuracy of the update to first order, it was shown numerically that augmenting the continuation algorithm with a second-derivative term can dramatically improve the accuracy of the update for practical applications. This conclusion is consistent with our previous findings [5].

11. Future Work

Additional work should target efficient and reliable application of the algorithm. Most importantly, an efficient and accurate method for estimating the tensor-vector products required for the derivative calculations must be developed and implemented. Once this is accomplished, more difficult test cases can be carried out, such as cases on finer grids and turbulent flows.

Additional considerations regarding the efficiency of the new algorithm for our applications include step-length adaptation algorithms and considerations for the linear solver.

Acknowledgments

The second author gratefully acknowledges financial assistance from the Natural Science and Engineering Research Council (NSERC), the Canada Research Chairs program, and the University of Toronto.

Computations were performed on the GPC supercomputer at the SciNet HPC Consortium. SciNet is funded by: the Canada Foundation for Innovation under the auspices of Compute Canada; the Government of Ontario; Ontario Research Fund - Research Excellence; and the University of Toronto.

References

- [1] Allgower, E. L., Georg, K., 1990. Introduction to Numerical Continuation Methods. Society for Industrial and Applied Mathematics.
- [2] Bischof, C., Carle, A., Corliss, G., Griewank, A., Hovland, P., 1991. ADIFOR - Generating derivative codes from Fortran programs. *Scientific Programming* 1, 1–29.
- [3] Brown, D. A., Zingg, D. W., June 2013. Advances in homotopy-based globalization strategies in computational fluid dynamics. AIAA-2013-2944.
- [4] Brown, D. A., Zingg, D. W., July 2014. A new monolithic homotopy continuation algorithm with CFD applications. In: Eighth International Conference on Computational Fluid Dynamics. Chengdu, China.
- [5] Brown, D. A., Zingg, D. W., 2016. Efficient numerical differentiation of implicitly-defined curves for sparse systems. *J. Comput. Appl. Math.* 304, 138–159.

- [6] Brown, D. A., Zingg, D. W., 2016. A monolithic homotopy continuation algorithm with application to computational fluid dynamics. *J. Comp. Phys.* 321, 55–75.
- [7] Carey, G. F., Krishnan, R., 1985. Continuation techniques for a penalty approximation of the Navier-Stokes equations. *Comput. Method. Appl. M.* 48, 265–282.
- [8] Carpenter, M. H., Gottlieb, D., Abarbanel, S., 1994. Time-stable boundary conditions for finite-difference schemes solving hyperbolic systems: methodology and application to high-order compact schemes. *J. Comput. Phys.* 111 (2), 220–236.
- [9] Del Rey Fernández, D. C., Hicken, J. E., Zingg, D. W., 2014. Review of summation-by-parts operators with simultaneous approximation terms for the numerical solution of partial differential equations. *Comput. Fluids* 95, 171–196.
- [10] Eisenstat, S. C., Walker, H. F., 1994. Globally convergent inexact Newton methods. *SIAM J. Optimiz.* 4, 393–422.
- [11] Fike, J. A., Alonso, J. J., 2011. The development of hyper-dual numbers for exact second-derivative calculations. AIAA 2011-866.
- [12] Funaro, D., Gottlieb, D., 1988. A new method of imposing boundary conditions in pseudospectral approximations of hyperbolic equations. *Math. Comput.* 51, 599–613.
- [13] Getz, N. H., 1995. Dynamic inversion of nonlinear maps with applications to nonlinear control and robotics. Ph.D. thesis, University of California at Berkeley, Berkeley, California, USA.
- [14] Hao, W., Hauenstein, J. D., Shu, C., Sommesse, A. J., Xu, Z., Zhang, Y., 2013. A homotopy method based on WENO schemes for solving steady state problems of hyperbolic conservation laws. *J. Comput. Phys.* 250, 332–346.
- [15] Hicken, J. E., Buckley, H., Osusky, M., Zingg, D. W., June 2011. Dissipation-based continuation: a globalization for inexact-Newton solvers. AIAA 2011-3237.
- [16] Hicken, J. E., Zingg, D. W., 2008. A parallel Newton-Krylov solver for the Euler equations discretized using simultaneous approximation terms. *AIAA J.* 46 (11), 2773–2786.
- [17] Hicken, J. E., Zingg, D. W., June 2009. Globalization strategies for inexact-Newton solvers. AIAA-2009-4139.
- [18] Jameson, A., Vassberg, J. C., Ou, K., 2012. Further studies of airfoils supporting non-unique solutions in transonic flow. *AIAA J.* 50 (12), 2865–2881.
- [19] Knoll, D. A., Keyes, D. E., 2004. Jacobian-free Newton-Krylov methods: a survey of approaches and applications. *J. Comput. Phys.* 193, 357–397.
- [20] Kreiss, H., Scherer, G., 1974. Finite element and finite difference methods for hyperbolic partial differential equations. In: de Boor, C. (Ed.), *Mathematical Aspects of Finite Elements in Partial Differential Equations: proceedings of a symposium conducted by the Mathematics Research Center, the University of Wisconsin*. Mathematics Research Center, the University of Wisconsin, Academic Press, pp. 195–212.
- [21] Liu, X.-D., Osher, S., Chan, T., 1994. Weighted essentially non-oscillatory schemes. *J. Comput. Phys.* 115 (1), 200–212.
- [22] Lomax, H., Pulliam, T. H., Zingg, D. W., 2001. *Fundamentals of Computational Fluid Dynamics*. Springer-Verlag.
- [23] Lyness, J. N., Moler, C. B., 1967. Numerical differentiation of analytic functions. *SIAM J. Numer. Anal.* 4 (2), 202–210.
- [24] Mackens, W., 1989. Numerical differentiation of implicitly defined space curves. *Computing* 41, 237–260.
- [25] McCroskey, W. J., October 1987. A critical assessment of wind tunnel results for the NACA 0012 airfoil. Tech. rep., Ames Research Center, Moffett Field, California, nASA TM 100019.
- [26] Nielsen, E. J., Anderson, W. K., Walters, R. W., Keyes, D. E., June 1995. Application of Newton-Krylov methodology to a three-dimensional unstructured Euler code. AIAA-95-1733.
- [27] Osusky, M., Zingg, D. W., 2013. A parallel Newton-Krylov-Schur flow solver for the Navier-Stokes equations discretized using summation-by-parts operators. *AIAA J.* 51 (12), 2833–2851.
- [28] Pönisch, G., Schwetlick, H., 1981. Computing turning points of curves implicitly defined by nonlinear equations depending on a parameter. *Computing* 26, 107–121.
- [29] Riley, D. S., Winters, K. H., 1990. A numerical bifurcation of natural convection in a tilted two-dimensional porous cavity. *J. Fluid Mech.* 215, 309–329.
- [30] Saad, Y., 2003. *Iterative Methods for Sparse Linear Systems*, 2nd Edition. SIAM, Philadelphia, PA.
- [31] Schwetlick, H., Cleve, J., 1987. Higher order predictors and adaptive steplength control in path following algorithms. *SIAM J. Numer. Anal.* 24 (6), 1382–1393.
- [32] Squire, W., Trapp, G., 1998. Using complex variables to estimate the derivatives of real functions. *SIAM Rev.* 40, 110–112.
- [33] Syam, M. I., Siyyam, H. I., 1999. Numerical differentiation of implicitly defined curves. *J. Comput. Appl. Math.* 108, 131–144.
- [34] Wagner, C. F., 2015. Improving shock-capturing robustness for higher-order finite element solvers. Master’s thesis, Massachusetts Institute of Technology, Cambridge, Massachusetts, United States.
- [35] Wales, C., Gaitonde, A. L., Jones, D. P., Avitabile, D., Champneys, A. R., 2012. Numerical continuation of high Reynolds number external flows. *Int. J. Numer. Meth. Fl.* 68 (2), 135–159.

- [36] Winters, K. H., 1987. A bifurcation study of laminar flow in a curved rectangular cross-section. *J. Fluid Mech.* 180, 343–369.
- [37] Yu, M., Wang, Z. J., 2016. Homotopy continuation of the high-order flux reconstruction/correction procedure via reconstruction (FR/CPR) method for steady flow simulation. *Comput. Fluids* 131, 16–28.